Flexural Design of Fibre-Reinforced Concrete

C Soranakom and B Mobasher

Department of Civil and Environmental Engineering, Arizona State University, USA

This is an original scientific paper published in Concrete Beton, journal of the Concrete Society of Southern Africa, in Volume 124, pp 6-15, March 2010.

Journal Contact Details:
PO Box 75364
Lynnwood Ridge
Pretoria, 0040
South Africa
+27 12 348 5305

admin@concretesociety.co.za
www.concretesociety.co.za

Flexural Design of Fibre Reinforced Concrete

by Chote Soranakom and Barzin Mobasher

Chote Soranakom is a post-doctoral fellow in the Department of Civil and Environmental Engineering at Arizona State University. His interests are in the area of fibre and fabric reinforced concrete materials and mechanical modelling of composite systems. **Barzin Mobasher** is a professor in the Department of Civil and Environmental Engineering at Arizona State University. He has more than 20 years of research experience in engineering materials. Mobasher is a member of American Concrete Institute committees 446, 544, and 549.

ABSTRACT: A set of closed form design equations for flexural design of fibre reinforced concrete are presented. These equations are based on simplified tensile and compressive constitutive response and may be used in a limit state approach or serviceability-based criterion that limits the effective tensile strain capacity. The equations allow generation of flexural moment-curvature response of a rectangular beam section for use in structural analysis calculations in addition to design charts for strain softening fibre reinforced concrete. To prevent sudden failure after flexural cracking and to control crack width, equations for minimum post-crack tensile strength are also proposed. The analytical tensile strain equations proposed for serviceability limit the average crack width of structural members. In addition, the bi-linear moment-curvature model is used in conjunction with geometrical relationship between curvature and deflection to determine short-term deflections of structural members. An example of a one-way slab demonstrates the calculation steps.

Keywords:

composite concrete flexural members; design; fibre reinforced concrete

INTRODUCTION

Fibre reinforced concrete (FRC) can be considered as a brittle matrix composite material consisting of cementitious matrix and discrete fibres. The fibres that are randomly distributed in the matrix act as crack arrestors. Once the matrix cracks under tension the debonding and pulling out of fibres dissipate energy, leading to a substantial increase in toughness[1]. The main areas of FRC applications are slabs on grade, tunnel linings, precast, and prestressed concrete products. Recently, elevated slabs of steel fibre-reinforced concrete (SFRC) have been successfully used where fibres provide the primary reinforcement[2,3]. A wide range of fibre-reinforced concrete systems including glass fibre-reinforced concrete (GFRC)[4], engineered cementitious composite (ECC)[5,6], slurry infiltrated concrete (SIFCON)[7,8], and high performance fibre reinforced concrete (HPFRC) [9,10] require better design guidelines. To standardise these materials, Naaman and Reinhardt[11] defined "strain-hardening" and "strain-softening" classifications based on tensile responses. Within the second category, additional terms of "deflection-hardening" and "deflection-softening" are defined to further classify the flexural response.

Despite the fact that FRC has been used in the construction industry for more than four decades, applications are still limited to a few market sectors. This is mainly due to the lack of standard guidelines for design procedures. To facilitate the design process, technical guidelines for FRC have been developed by RILEM committee TC162-TDF for SFRC [12,13,14,15,16] during the past 15 years. The committee proposed three-point bending test of a notched beam specimen for material characterisation. The elastically equivalent flexural strength at specific crack mount opening displacement (CMOD) is empirically related to the tensile stress-strain model. The compression response is described by a parabolic-rectangular stress strain model. The strain compatibility analysis of a layered beam cross section is required to determine the ultimate moment capacity. Similar to the RILEM, German guidelines for design of flexural members use the strain compatibility analysis to determine the moment capacity[17]. In the UK[18], the practice of FRC traditionally followed the Japanese Standard JCI-SF4 (1984)[19]; however, it has recently shifted towards the RILEM design methodology. The Italian guideline is also based on load-deflection curves deduced from flexural or direct tension test [20]. The current US design guidelines for flexural members are based on empirical equations of Swamy et al.[21,22]. Particular type of fibres and nature of concrete were not specified in the guidelines. Henager and Doherty[23] proposed a tensile stress block for SFRC that is comparable with the ultimate strength design of ACI 318-05[24].

This paper proposes a design methodology for strain-softening FRC and consists of two parts: design for ultimate strength and design for serviceability. The design procedures are based on theoretical derivations of Soranakom and Mobasher[25,26], in addition to ACI 318-05[24] and RILEM TC 162-TDF[16]. Topics include nominal moment capacity; minimum post crack tensile strength for flexural cracking; tensile strain limit; short term deflection calculations, and a conversion design chart to correlate traditional reinforced concrete and FRC systems.

A design example of one-way slab is presented to illustrate the use of equations in design of typical structural members.

STRAIN-SOFTENING FRC MODEL

Tensile and compressive response of strain-softening FRC such as steel and polymeric fibre-reinforced concrete (SFRC and PFRC) can be simplified to idealized stress strain models as shown in Fig. 1(a)&(b). In these materials the contribution of fibres is mostly apparent in the post peak tensile region, where the response is described by a decaying stress strain relationship. It is however possible to assume an average constant post crack tensile strength σ_p for the softening response, which can be correlated to the fibre volume fraction and their bond characteristics[21-23].

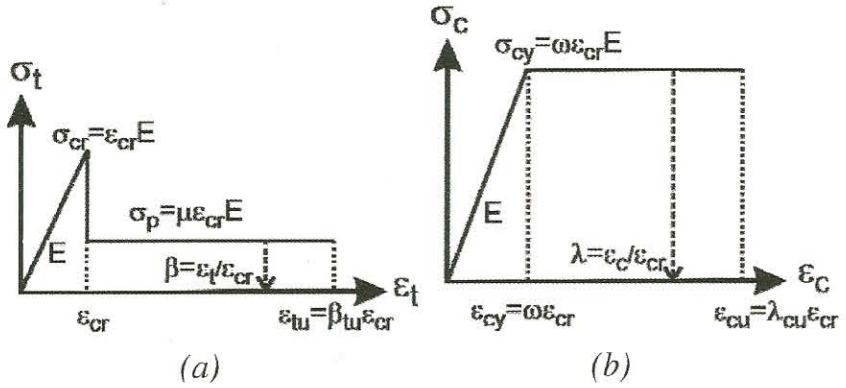

Fig 1 - Idealised material modelss for strain-softening fibre - reinforced cocrete: (A) Tension model; and (b) compression model

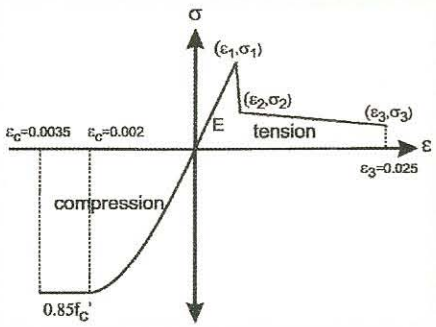

Fig 2 Idealised material models for strain-softening fibre-reinforced concrete: (a) tension model; and (b) compression model.

The following assumptions are made in the development of the material models: a) Young's modulus E for compression and tension are equal, b) tension model [Fig. 1(a)] consists of a linear stress strain response up to the cracking tensile strain ε_{cr}, followed by a constant post crack tensile strength $\sigma_p = \mu E\varepsilon_{cr}$ with parameter μ $(0 \le \mu \le 1)$ representing the post crack strength as a fraction of the cracking tensile strength $\sigma_{cr} = E\varepsilon_{cr}$, and c) compression model defined by an elastic perfectly plastic model [Fig. 1(b)] using a yield compressive strain $\varepsilon_{cy} = \omega\varepsilon_{cr}$ with a parameter ω $(\omega \ge 1)$ representing the compressive to cracking tensile strain ratio.

Study of material parameters[25] reveals that the ultimate moment capacity of FRC is significantly affected by the normalised post crack tensile strength parameter m while less sensitive to the compressive to tensile strength ratio w. In order to minimize the number of material parameters, the tensile strength and Young's modulus are assumed to be marginally affected by fibre type and content and conservatively estimated by the relationship governing normal concrete using ACI-318 Sec. 11.2 and Sec. 8.5.1, respectively.

$$\sigma_{cr} = E\varepsilon_{cr} = 0.56\sqrt{f_c'} \quad \text{(MPa)}$$
$$\left(\text{or } = 6.7\sqrt{f_c'} \quad \text{(psi)}\right) \qquad (1)$$

$$E = 4{,}733\sqrt{f_c'} \quad \text{(MPa)}$$
$$\left(\text{or } = 57{,}000\sqrt{f_c'} \quad \text{(psi)}\right) \qquad (2)$$

where f_c' is the ultimate uniaxial cylinder compressive strength. First crack tensile strain for FRC can be calculated assuming Hooke's law as:

$$\varepsilon_{cr} = \frac{\sigma_{cr}}{E} = \frac{0.56\sqrt{f_c'}}{4733\sqrt{f_c'}} = \frac{6.7\sqrt{f_c'}}{57000\sqrt{f_c'}} = 118\ \mu\text{str} \qquad (3)$$

According to the RILEM model[16] shown in Fig. 2, the ultimate tensile strain ε_3 is defined as 0.025. The ultimate compressive strain ε_{cu} is limited to 0.0035, which is the lower bound value of typical SFRC[27,28] ,and the yield compressive strength for FRC is adopted as:

$$\sigma_{cy} = 0.85f_c' \quad \text{(MPa and psi)} \qquad (4)$$

The two normalised parameters used in the material models [Fig. 1(a)&(b)] are summarised as follows:

$$\mu = \frac{\sigma_p}{E\varepsilon_{cr}} = \frac{\sigma_p}{\sigma_{cr}} \qquad (5)$$

$$\omega = \frac{\varepsilon_{cy}}{\varepsilon_{cr}} = \frac{\sigma_{cy}}{E\varepsilon_{cr}} = \frac{\sigma_{cy}}{\sigma_{cr}} = 1.52\sqrt{f_c'} \quad \text{(Slunit)}$$
$$\left(\text{or } \ 0.127\sqrt{f_c'} \quad \text{(US customary unit)}\right) \qquad (6)$$

Note that the coefficients 1.52 and 0.127 used in Eq. (6) are for f_c' expressed in MPa and psi, respectively. Equation (6) implies that the normalised yield compressive strain ω is also a compressive to tensile strength ratio.

Research significance of reinforced concrete

The proposed design guideline provides computational efficiency over the commonly used strain compatibility analysis of a layered beam in determining moment capacity of FRC members.

The closed form equations and guidelines are compatible with the ACI-318 design method procedures while allowing deflection and serviceability criteria to be calculated, based on fundamentals of structural mechanics.

These computations allow engineers to reliably design and compare the overall performance of conventional reinforced concrete system and FRC.

Thus, these terms can be used interchangeably. For typical f_c' between 20 and 65 MPa, ω varies between 6.8 and 12.8. The tensile and compressive responses terminate at the normalised ultimate tensile strain b_{tu} and compressive strain λ_{cu} respectively.

$$\beta_{tu} = \frac{\varepsilon_{tu}}{\varepsilon_{cr}} = \frac{0.025}{118\times10^{-6}} \approx 212 \quad (7)$$

$$\lambda_{cu} = \frac{\varepsilon_{cu}}{\varepsilon_{cr}} = \frac{0.0035}{118\times10^{-6}} \approx 30 \quad (8)$$

Note that the terms β and λ without subscript refer to normalised tensile strain ($\varepsilon_t / \varepsilon_{cr}$) and compressive strain ($\varepsilon_c / \varepsilon_{cr}$), respectively and are functions of imposed curvature on a section.

Moment curvature response

For a rectangular section, the derivations for neutral axis depth ratio *k*, normalised moment *m*, and normalised curvature ϕ are described in an earlier publication[25]. Fig. 3 shows 3 ranges of applied top compressive strain $0 \le \varepsilon_c \le \varepsilon_{cr}$, $\varepsilon_{cr} \le \varepsilon_c \le \varepsilon_{cy}$ and $\varepsilon_{cy} \le \varepsilon_c \le \varepsilon_{cu}$ or in dimensionless form $0 \le \lambda \le 1$, $1 \le \lambda \le \omega$ and $\omega \le \lambda \le \lambda_{cu}$.

The location of neutral axis parameter *k* is derived by solving the equilibrium of internal forces. The moment was computed from taking the force about the neutral axis, while the curvature is obtained by dividing top compressive strain with the depth of neutral axis. The corresponding closed form solutions for normalised neutral axis, moment and curvature (*k*, *m*, ϕ) are presented in Table 1. Using these expressions, the moment *M* and curvature Φ represented in terms of their first cracking values (M_{cr} and Φ_{cr}) are defined as:

$$M = mM_{cr};\quad M_{cr} = \frac{\sigma_{cr} b h^2}{6} \quad (9)$$

Range	k	m	ϕ
$0 \le \lambda \le 1$	$\frac{1}{2}$	$\frac{\lambda}{2k}$	$\frac{\lambda}{2k}$
$1 \le \lambda \le \omega$	$\frac{2\mu\lambda}{\lambda^2 + 2\mu(\lambda+1) - 1}$	$\frac{(2\lambda^3 + 3\mu\lambda^2 - 3\mu + 2)k^2}{\lambda^2} - 3\mu(2k-1)$	
$\omega \le \lambda \le \lambda_{cu}$	$\frac{2\mu\lambda}{-\omega^2 + 2\lambda(\omega+\mu) + 2\mu - 1}$	$\frac{(3\omega\lambda^2 - \omega^3 + 3\mu\lambda^2 - 3\mu + 2)k^2}{\lambda^2} - 3\mu(2k-1)$	

Table 1-Neutral axis depth ratio and normalised moment curvature expression for three ranges of applied normalised top comprehensive strain λ.

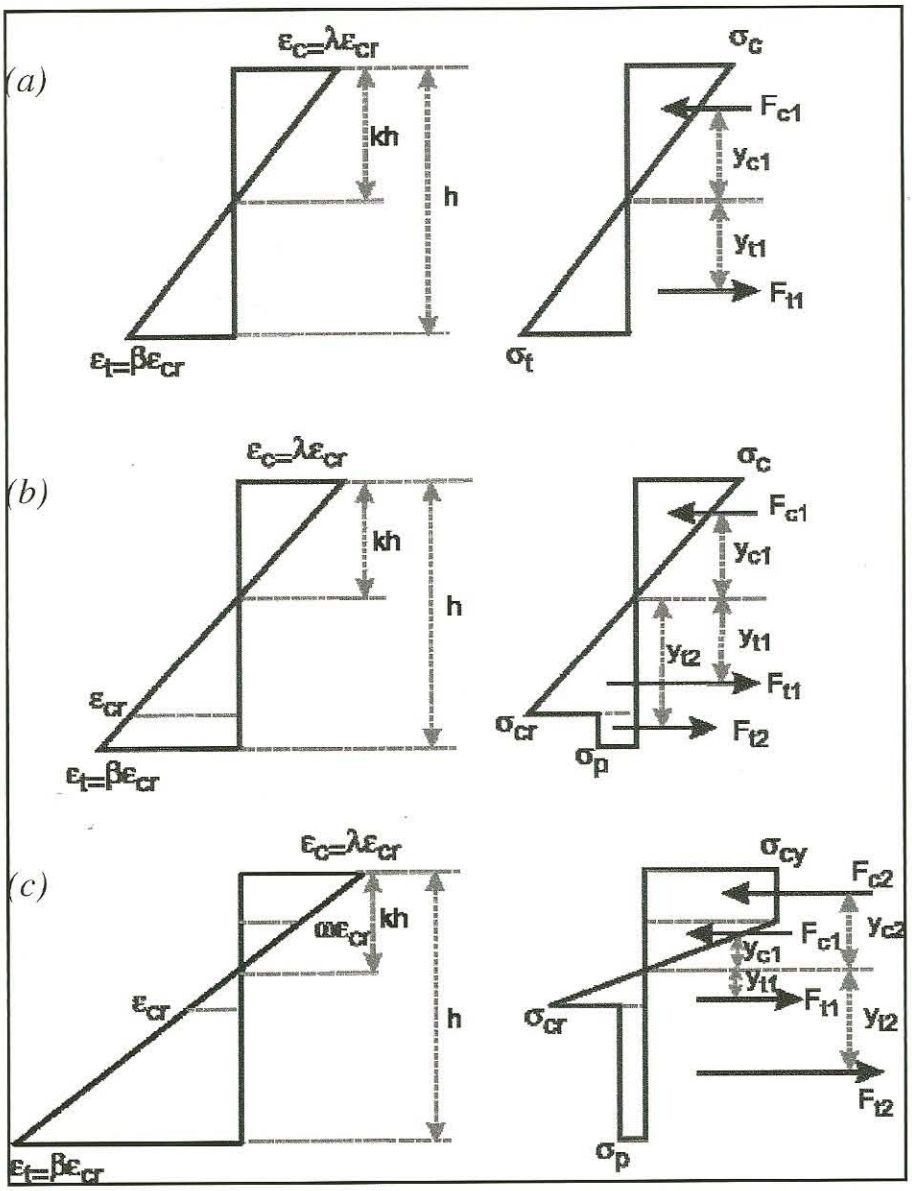

Figure 3-Stress-strain diagram at three ranges of normalised top comprehensive strain λ:(a) elastic for comprehension and tension (0 < λ ≤); (b) elastic for comprehension but nonlinear for tension (1 < λ ≤ω); (c) plastic for compression and nonlinear for tension (λ>ω).

$$\Phi = \phi\,\Phi_{cr};\quad \Phi_{cr} = \frac{2\varepsilon_{cr}}{h} \quad (10)$$

where *b* and *h* are width and height of beam, respectively.

The moment capacity at ultimate compressive strain ($\lambda = \lambda_{cu}$) is very well approximated by the limit case of ($\lambda = \infty$). Using the expression for k in range 3 of Table 1, one obtains the neutral axis parameter at infinity k_∞.[25]

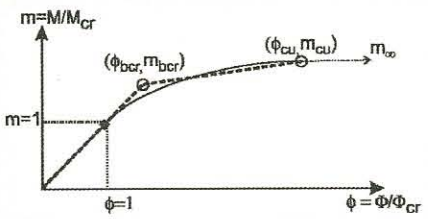

Figure 4-Normalised moment curvature response for strain-softening deflection-hardening material and it is simplified bilinear model.

ALLOWABLE TENSILE STRAIN

$$k_\infty = \frac{\mu}{\omega+\mu} \quad (11)$$

By substituting $k = k_\infty$ and $\lambda = \infty$ in the expression for m in range 3 of Table 1, the ultimate moment capacity, m_∞ is also obtained

$$m_\infty = \frac{3\omega\mu}{\omega+\mu} \quad (12)$$

BI-LINEAR MOMENT-CURVATURE DIAGRAM

For sufficiently high post peak tensile capacity, the flexural response of FRC shows no drop in moment capacity after cracking and is referred to as strain-softening deflection-hardening.

Fig. 4 shows a typical moment-curvature response for this class of material generated from Table 1. The smooth response can be approximated as a bilinear response using an optimization approach in the curve fitting.

The termination point of the bi-linear model was designated as m_{cu} and assumed to be equal to m_∞ given by Eq. (12). The intersection point is defined as the bilinear cracking point (ϕ_{bcr}, m_{bcr}) and is higher than the original cracking point (ϕ_{cr}, m_{cr}). With the predetermined bi-linear cracking points from material database covering possible range of FRC,[25,29] a linear regression equation was established as:

$$m_{bcr} = 0.743 m_{cu} + 0.174 \quad \text{and} \quad \phi_{bcr} = m_{bcr} \quad (13)$$

The curvature at the ultimate compressive strain ϕ_{cu} can be determined by substituting a relatively large λ_{cu} value in the expression for k and ϕ in range 3 presented in Table 1. For example a simplified expression for ϕ_{cu} at λ_{cu} =30 is:

$$\phi_{cu} = \frac{-\omega^2 + 60\omega + 62\mu - 1}{4\mu} \quad (14)$$

The bilinear model can be used to obtain the curvature distribution according to a given moment profile. The slope in the elastic part is $\phi_{br}/m_{br} = 1$ while the slope in the post crack region is

$$\theta_{pcr} = \frac{\phi_{cu} - \phi_{bcr}}{m_{cu} - m_{bcr}} \quad (15)$$

Finally, the normalised curvature-moment relationship can be expressed as:

$$\phi = \begin{cases} m & \text{for } 0 < m \le m_{bcr} \\ \phi_{bcr} + \theta_{pcr}(m - m_{bcr}) & \text{for } m > m_{bcr} \end{cases} \quad (16)$$

For sufficiently high fibre volume fractions and a good bond property, the ultimate moment capacity of the strain-softening FRC can be as high as 2.6 times the first cracking moment[25]. There may however be a need to design based on a limit to the allowable tensile strain and crack width.

Since many deflection-hardening FRCs show multiple cracking, the nominal tensile strain averaged from several cracks spaced apart is proposed as the serviceability criterion. This section only addresses the effect of lower and upper bounds of the allowable tensile limit and their effect on service moments.

From the linear strain diagrams in the post crack ranges [Fig. 3(b)&(c)], the relationship between normalised allowable tensile strain β_a and the corresponding normalised compressive stain λ_a at a balanced condition can be written as:

$$\frac{\lambda_a \varepsilon_{cr}}{kh} = \frac{\beta_a \varepsilon_{cr}}{h - kh} \quad (17)$$

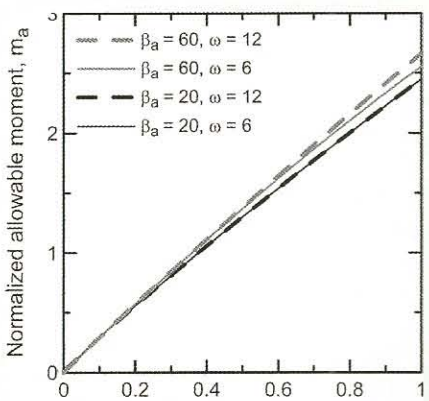

Figure 5 Normalized post crack tensile strain, μ

Table 3-Steel fibre reinforced concrete parameters for RILEM model.

Mixture	W_f, kg/m^3 (lb/yd^3)	E, MPa (psi)	f'_c, MPa (psi)	σ_1, MPa (psi)	σ_2, MPa (psi)	σ_3, MPa (psi)	ε_1, %	ε_2, %	ε_3, %
NSC	25 (42)	31,854 (4.62E + 06)	30.2 (4380)	3.5 (508)	1.1 (160)	0.8 (116)	0.011	0.21	25
NSC	50 (84)	30,564 (4.43E + 06)	26.6 (3858)	4.2 (609)	2.0 (290)	1.2 (174)	0.014	0.24	25
HSC	60 (101)	38,411 (5.57E + 06)	52.9 (7673)	6.2 (899)	3.1 (450)	3.1 (450)	0.016	0.26	25

Note: Strain at compressive yield stress $\varepsilon_{cy} = 0.133\%$, and ultimate compressive strain $\varepsilon_{cu} = 0.35\%$ for all mixtures.

Table 2-Normalised allowable moment.

Range		ω = 6	ω = 12
m_{2a} $1 \le \lambda \le \omega$	$\beta_a = 20$	$\frac{76\mu\sqrt{38\mu+1} + 2\sqrt{38\mu+1} + 1197\mu + 2}{(20 + \sqrt{38\mu+1})^2}$	
	$\beta_a = 60$	$\frac{236\mu\sqrt{118\mu+1} + 2\sqrt{118\mu+1} + 10{,}797\mu + 2}{(60 + \sqrt{118\mu+1})^2}$	
m_{3a} $\omega \le \lambda \le \lambda_{cu}$	$\beta_a = 20$	$\frac{18(1444\mu^2 + 12{,}388\mu - 343)}{(277 + 38\mu)^2}$	$\frac{36(1444\mu^2 + 30{,}172\mu - 6591)}{(625 + 38\mu)^2}$
	$\beta_a = 60$	$\frac{18(13{,}924\mu^2 + 95{,}108\mu - 343)}{(757 + 118\mu)^2}$	$\frac{36(13{,}924\mu^2 + 206{,}972\mu - 6591)}{(1585 + 118\mu)^2}$

Equation (17) is solved in conjunction with the neutral axis parameter k defined in Table 1 for two possible ranges 2 or 3. This results in two possibilities of λ_a:

$$\lambda_a = \begin{cases} \sqrt{2\mu\beta_a - 2\mu + 1} & \text{for } \beta_a \le \beta_{crit} \\ \dfrac{2\mu\beta_a - 2\mu + \omega^2 + 1}{2\omega} & \text{for } \beta_a > \beta_{crit} \end{cases} \quad (18)$$

$$\beta_{crit} = \frac{\omega^2 + 2\mu - 1}{2\mu} \quad (19)$$

where β_{crit} is the critical tensile strain. When $\beta_a \le \beta_{crit}$ the parameter λ_a will be in between 1 and ω (range 2) and when $\beta_a > \beta_{crit}$, the parameter λ_a will be greater than β_a range 3.

Two levels of normalised allowable tensile strain β_a = 20 and 60 (corresponding to 2360 and 7080 mstr for the cracking strain of 118 mstr defined in Eq. (3)) and the lower and upper bound compressive tensile strength ratio ω = 6 and 12 are evaluated. The closed form solutions for the allowable moments corresponding the combination of these β_a and ω can be derived by first substituting the values in Eq. (18), then substituting the obtained λ_a and/or ω in the expressions for k and m in range 2 and 3 in Table 3. The final form of allowable moments in range 2 or 3 (m_{2a} and m_{3a}) are presented in Table 2 depending on the value of β_a compared to β_{crit} as shown in Eq. (19).

Fig. 5 presents normalised allowable moment for post crack tensile strain β in the range of 0.0 - 1.0. The increase in allowable tensile strain β_a from 20 to 60 for each level of w slightly increases the allowable moment, with the maximum difference of only 8.8% at μ = 1.0. Thus, use of lower bound value β_a = 20 as a tensile strain criterion is reasonably safe for preventing excessive cracking while the moment capacity is slightly reduced. Note that at β_a = 20, the allowable moment is insensitive to changes of ω between 6 and 12, while at β_a = 60, only small differences are observed.

Based on this simplification, a conservative case of β_a = 20 and ω = 6 as presented in Table 2 is proposed as a tensile strain criterion and summarised as: (see top of page)

$$m_a = \begin{cases} \dfrac{76\mu\sqrt{38\mu+1} + 2\sqrt{38\mu+1} + 1197\mu + 2}{\left(20 + \sqrt{38\mu+1}\right)^2} & \text{for } \beta_a = 20 \le \dfrac{35+2\mu}{2\mu} \\ \dfrac{18\left(1444\mu^2 + 12388\mu - 343\right)}{(277+38\mu)^2} & \text{for } \beta_a = 20 > \dfrac{35+2\mu}{2\mu} \end{cases} \quad (20)$$

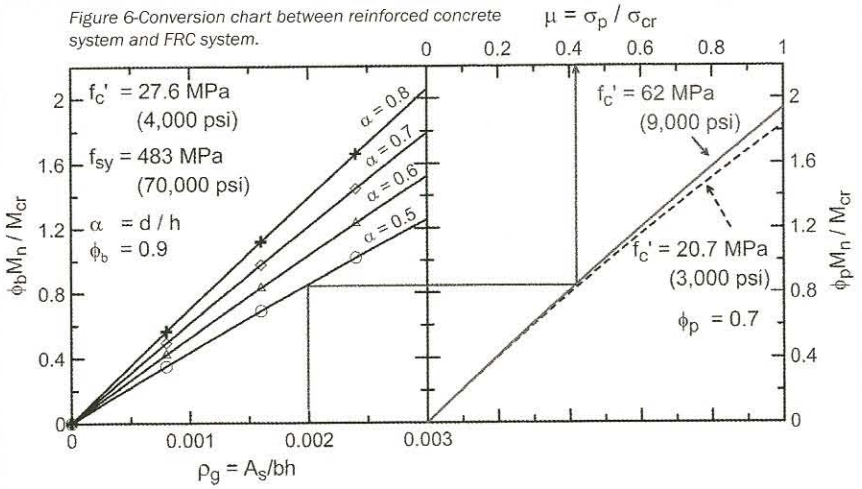

Figure 6-Conversion chart between reinforced concrete system and FRC system.

(a) reinforced concrete *(b) fiber-reinforced concrete*

ULTIMATE MOMENT CAPACITY

Load and resistance factor design (LRFD) is based on the reduced nominal moment capacity $\phi_p M_n$ exceeding the ultimate factored moment M_u that is determined by linear elastic analysis and load coefficients in accordance to ACI 318-05 Sec 9.2. The reduction factor ϕ_p addresses the uncertainty of using post crack tensile strength in predicting ultimate moment capacity. Based on the statistical analysis of limited test data[29] a value ϕ_p = 0.7 was used in this study. The nominal moment capacity M_n can be obtained by using Eqs. (9)&(12) with the reduction factor: Alternatively, the nominal moment capacity can be expressed as a function of post crack tensile strength m and compressive strength ϕ_c' by substituting Eq. (6) in (21).

The post crack tensile strength necessary to carry the ultimate moment can be obtained from Eq. (22) as:

Strain-softening FRC has therefore a moment capacity that ranges between 1.0 and 2.6 times the cracking moment (Fig. 5); therefore, it is suitable for slab applications where internal moment is relatively low compared to the cracking moment and shear is generally not critical.

For higher internal moment such as beams in structure, the use of fibres may not be sufficient and require additional rebar to increase the capacity.

The design of this flexural member is presented in reference[29] while shear capacity of using fibre-reinforced concrete can be found in literature[30,31].

$$\phi_p M_n = \phi_p m_\infty M_{cr} = \frac{3\omega\mu}{\omega+\mu}\phi_p M_{cr} \ge M_u \quad (21)$$

$$\phi_p M_n = \left[\frac{6\mu\sqrt{f_c'}}{\xi\mu + 2\sqrt{f_c'}}\right]\phi_p M_{cr} \quad (\xi = 1.32 \text{ for } f_c' \text{ in MPa, } \xi = 15.8 \text{ for } f_c' \text{ in psi}) \quad (22)$$

$$\mu = \frac{2M_u\sqrt{f_c'}}{6\phi_p M_{cr}\sqrt{f_c'} - \xi M_u} \quad (\xi = 1.32 \text{ for } f_c' \text{ in MPa, } \xi = 15.8 \text{ for } f_c' \text{ in psi}) \quad (23)$$

Minimum Post Crack Tensile Capacity for Flexure

To prevent a sudden drop of moment capacity after initial cracking, a minimum fibre dosage is required. The post crack tensile strength that maintains a load capacity equivalent to the cracking strength level ($M_n = M_{cr}$) is defined as m_{crit} and obtained by solving Eq. (21) with a reduction factor $\phi_p = 1$.

$$\mu_{crit} = \frac{\omega}{3\omega - 1} \qquad (24)$$

For typical FRC materials with compressive to tensile strain ratio ω ranging from 6 - 12 results in μ_{crit} = 0.353 - 0.343. A conservative value of $\mu_{mim,flex}$ = 0.35 therefore ensures post crack moment capacity higher than the first cracking moment.

Beam	Mixture	W_f, kg/m^3 (lb/yd^3)	L, m (ft)	S_{mid}, m (ft)	P_{max}, kN (kip)	$M_{u,exp}$, kN-m (kip-ft)	M_n, kN-m (kip-ft)
B1	NSC	25 (42)	1.0 (3.33)	0.2 (8.0)	26.7 (6.0)	5.34 (3.94)	4.25 (3.13)
B2	NSC	25 (42)	2.0 (6.67)	0.2 (8.0)	10.3 (2.3)	4.64 (3.42)	4.25 (3.13)
B3	NSC	50 (84)	1.0 (3.33)	0.2 (8.0)	27.1 (6.1)	5.42 (4.00)	7.44 (5.49)
B4	NSC	50 (84)	2.0 (6.67)	0.2 (8.0)	16.9 (3.8)	7.61 (5.61)	7.44 (5.49)
B5	HSC	60 (101)	1.0 (3.33)	0.2 (8.0)	63.4 (14.3)	12.68 (9.35)	11.71 (8.64)
B6	HSC	60 (101)	2.0 (6.67)	0.2 (8.0)	21.5 (4.8)	9.68 (7.14)	11.71 (8.64)

Table 5-Comparison of ultimate moment capacity obtained by test results and design equations.

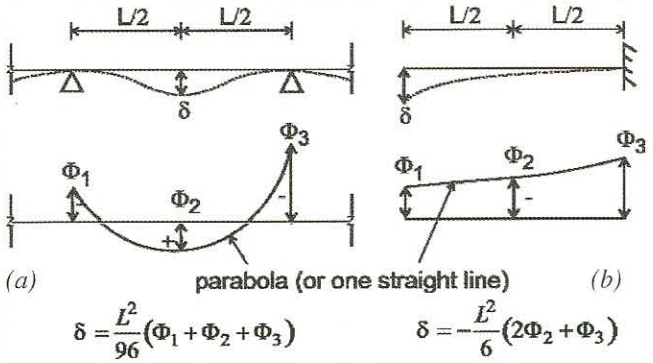

Figure 7-Geometric relationship between curvature and deflection[32,33].

Conversion Design Chart

An equivalent flexural FRC system can be substituted for minimum reinforcement in reinforced concrete structures. A conversion design chart is presented to help designers replace the reinforced concrete system with FRC system that has the same flexural capacity. The nominal moment capacity of a single reinforced concrete section can be determined by the compressive stress block concept (ACI Sec 10.2.7)

$$M_n = A_s f_y \left(d - \frac{a}{2} \right) \qquad (25)$$

where $a = A_s f_y / (0.85 f_c' b)$ is the depth of compressive stress block, $A_s = \rho_g bh$ is the area of tensile steel, ρ_g is the reinforcement ratio per gross section bh, and a is the normalised effective depth (d/h). The reduction factors ϕ_b = 0.9 and ϕ_p = 0.70 are used in the conversion chart to address the reliability of two reinforcing mechanisms. For any grade of steel and concrete strength, a conversion chart can be generated by Eqs. (22) and (25) as shown by Fig. 6.

The reinforcement ratio ρ_g together with the normalised effective depth *a* determine the moment capacity of the reinforced concrete system in Fig. 6(a) which can be transferred to the FRC chart to obtain normalised post crack tensile strength m in Fig. 6(b).

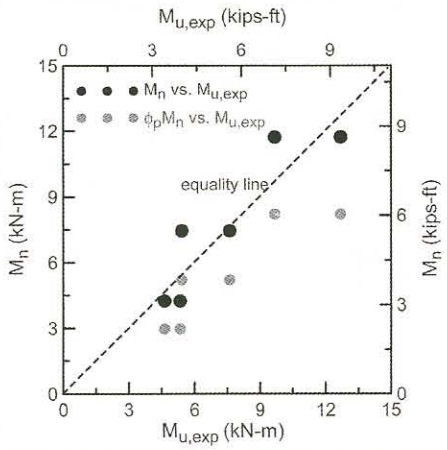

Figure 8-Predicted nominal moment capacity versus expreimental ultimate moment.

Table 4—Equivalent steel FRC parameters for the proposed model

Mixture	W_f, kg/m^3 (lb/yd^3)	σ_{cy}, MPa (psi)	σ_{cr}, MPa (psi)	σ_p, MPa (psi)	ω	μ	m_∞	b, m (in.)	h, m (in.)	M_{cr}, kN-m (kip-ft)	M_n, kN-m (kip-ft)
NSC	25 (42)	30.2 (4381)	3.5 (508)	1.1 (160)	8.63	0.31	0.91	0.2 (8.0)	0.2 (8.0)	4.67 (3.44)	4.25 (3.13)
NSC	50 (84)	26.6 (3858)	4.2 (609)	2.0 (290)	6.33	0.48	1.33	0.2 (8.0)	0.2 (8.0)	5.60 (4.13)	7.44 (5.49)
HSC	60 (101)	52.9 (7673)	6.2 (899)	3.1 (450)	8.53	0.50	1.42	0.2 (8.0)	0.2 (8.0)	8.27 (6.10)	11.71 (8.64)

Note: Strain at compressive yield stress ε_{cy} = 0.133%, and ultimate compressive strain ε_{cu} = 0.35 % for all mixtures.

Deflection calculation for serviceability

An important aspect of serviceability-based design is in accurate calculation of deflections under service load. The present approach can be used to compute the deflections by integration of the curvature along the beam length. Geometric relationship between curvature and deflection have been derived by Ghali[32,33]. The curvature distribution along the length can be arbitrary; however, a parabolic or linear shape result in accurate results while other shapes result in approximate values.

The sign convention for curvature is the same as the convention used for moments. Two typical cases of a simple beam (or continuous beam) and cantilever beam are presented in Fig. 7. The mid span deflection d of a simple (or continuous beam) can be computed by:

$$\delta = \frac{L^2}{96}(\Phi_1 + \Phi_2 + \Phi_3) \quad (26a)$$

The tip deflection of the cantilever beam can be computed by:

$$\delta = -\frac{L^2}{6}(2\Phi_2 + \Phi_3) \quad (26b)$$

where L is the span length, and Φ_1, Φ_2, and Φ_3 are the curvature at left end, centre, and right end, respectively. For short term deflection, the curvatures Φ_1 - Φ_3 due to moment at service loads can be estimated from Eqs. (10)&(16).

Model Prediction

Full scale beam tests from the Brite Eiram project BRPR-CT98-0813 "Test and design methods for steel fibre reinforced concrete" were used in the model verification[34]. The first set of the experimental programme studied the effects of concrete strength, fibre dosage, and span length on SFRC beams.

Two grades of normal strength concrete (NSC) and high strength concrete (HSC) were used. Normal strength concrete used the fibre type RC 65/60 BN at 25 and 50 kg/m^3 (42.1 and 84.3 lb/y^3) while HSC used fibre type RC 80/60 BP at 60 kg/m^3 (101.1 lb/y^3). Two span lengths of 1.0 and 2.0 m (3.33 and 6.67 ft) were used for the same cross section of 0.20 x 0.20 m (8 x 8 in). Two replicate samples were tested under four point bending for each span length while the spacing between the two point loads was kept constant at 0.2 m (8 in).

Material properties were characterized according to the RILEM model as shown in Fig. 2 and presented in Table 3. Key strength parameters used in the design were computed as shown in Table 4: $\sigma_{cy} = 0.85 f_c'$, $\sigma_{cr} = \sigma_1$, $\sigma_p = (\sigma_2 + \sigma_3)/2$. Using these definitions μ, ω, M_{cr}, and m_∞, can be calculated by Eqs. (5), (6), (9), and (12), respectively. Nominal moment capacity M_n can be calculated by Eq. (21) with $\phi_p = 1$. Note that Eq. (21) was used instead of (22) since $\omega = 0.85 f_c'/\sigma_1$ was obtained directly from Table 3. On the contrary, Eq. (22) ignores s_1 by assuming $\sigma_{cr} = 0.56 f_c'^{0.5}$ (or $6.7 f_c'^{0.5}$) and defines $\omega = 0.85 f_c/\sigma_{cr} = 1.53 f_c'^{0.5}$ (or $0.127 f_c'^{0.5}$). Table 5 presents the average test results of two replicates of the six beams (B1-B6) series for three mixtures and two span lengths.

To compare the test results with the nominal moment capacity M_n, ultimate moment of the section $M_{u,exp}$ was calculated from the maximum experimental load P_{max}.

$$M_{u,exp} = \frac{P_{max}(L - S_{mid})}{4} \quad (27)$$

where L is the clear span and S_{mid} is the spacing between the load points defined earlier. The experimental capacity $M_{u,exp}$ was compared to the proposed nominal moment capacity M_n in Fig. 8 and they show good agreement with some variation. By using the recommended reduction factor ϕ_p of 0.7, the reduced moment capacity $\phi_p M_n$ is obtained well below the experimentally obtained values [29].

Design examples

The design procedure for FRC is best suited for thin structural applications such as slabs and wall systems since size effect is minimal and the applied moment is relatively low compared to the cracking moment.

An example is presented to demonstrate the design calculations for a one-way slab with a single span of 3.5 m (11.67 ft) subjected to a uniformly distributed live load of 2.0 kN/m^2 (41.8 lb/ft^2) and superimposed dead load of 0.7 kN/m^2 (14.6 lb/ft^2). A point load of 4.0 kN/m (0.274 kips/ft) is applied at the centre. The design requires use of SFRC with a compressive strength ϕ_c' of 45 MPa (6531 psi) and unit weight of 24 kN/m^3 (153 lb/ft^3).

Ultimate moment capacity

The one-way slab is designed based on 1.0 m strip (3.33 ft). The self weight for an assumed thickness of 0.15 m (6 in) is:

$$w_{sw} = 0.15 \times 24 = 3.6\ kN/m^2 \quad (75.2\ lb/ft^2)$$

The factored loads according to ACI Sec. 9.2.1 are

$$w_u = 1.2(3.6 + 0.7) + 1.6(2.0) = 8.36\ kN/m^2 \quad (174.6\ lb/ft^2)$$

$$P_u = 1.6(4.0) = 6.4\ kN/m \quad (0.439\ kips/ft)$$

The maximum moment at mid span due to the uniform and point loads

$$M_u = \frac{w_u L^2}{8} + \frac{P_u L}{4} = \frac{8.36 \times 3.5^2}{8} + \frac{6.4 \times 3.5}{4}$$

$$= 18.4\ kN\text{-}m/m \quad (4.14\ kip\text{-}ft/ft)$$

Tensile strength and cracking moment are estimated by Eqs. (1)&(9), respectively.

$$\sigma_{cr} = 0.56\sqrt{45} = 3.75\ MPa \quad (544\ psi)$$

$$M_{cr} = \frac{\sigma_{cr} b h^2}{6} = \frac{(3.75 \times 10^3) \times 1.0 \times 0.15^2}{6}$$

$$= 14.06\ kN\text{-}m/m \quad (3.16\ kips\text{-}ft/ft)$$

The required post crack tensile strength for the ultimate moment M_u by Eq. (23) is:

$$\mu = \frac{2M_u\sqrt{f_c'}}{6\phi_p M_{cr}\sqrt{f_c'} - \xi M_u}$$

$$= \frac{2 \times 18.4\sqrt{45}}{6 \times 0.7 \times 14.06\sqrt{45} - 1.32 \times 18.4} = 0.66$$

$$= 0.66$$

Check tensile strain limit

The post crack tensile strength is determined by Eq. (1), $\sigma_p = \mu\sigma_{cr} = 0.66 \times 3.75 = 2.48$ MPa(360 psi)

Since the allowable tensile strain $\beta_a = 20 > (35 + 2 \times 0.66) / (2 \times 0.66) = 27.5$ in Eq. (20), the allowable moment is calculated as:

$$m_a = \frac{18(1444\mu^2 + 12388\mu - 343)}{(277 + 38\mu)^2}$$

$$= \frac{18(1444\times 0.66^2 + 12388\times 0.66 - 343)}{(277 + 38\times 0.66)^2} = 1.67$$

Unfactored loads are used to calculate the moment at service condition at the mid span.

$$M_s = \frac{wL^2}{8} + \frac{PL}{4} = \frac{(3.6 + 0.7 + 2.0)\times 3.5^2}{8} + \frac{4.0\times 3.5}{4}$$

$$= 13.15 \text{ kN-m/m } (2.96 \text{ kips-ft/ft})$$

The normalised moment at service load is

$$m_s = \frac{M_s}{M_{cr}} = \frac{13.15}{14.06} = 0.935 \quad < m_a = 1.67 \Rightarrow \text{"passed"}$$

Short term deflection

In order to calculate the deflection, the bilinear curvature-moment relationship is generated. The compressive to tensile strength ratio w computed by Eq. (6) is:

$$\omega = 1.52\sqrt{f_c'} = 1.52\sqrt{45} = 10.2$$

Two data points (ϕ_{br}, m_{br}) and (ϕ_{cu}, m_{cu}), and the slope θ_{pcr} in the post crack region can be determined by Eqs. (12)-(16).

$$m_{cu} = m_\infty = \frac{3\omega\mu}{\omega + \mu} = \frac{3\times 10.2\times 0.66}{10.2 + 0.66} = 1.86$$

$$\phi_{cu} = \frac{-\omega^2 + 60\omega + 62\mu - 1}{4\mu}$$

$$= \frac{-10.2^2 + 60\times 10.2 + 62\times 0.66 - 1}{4\times 0.66} = 207.5$$

$$m_{bcr} = 0.743 m_u + 0.174 = 0.743\times 1.86 + 0.174 =$$

$$= 1.56$$

$$\phi_{bcr} = m_{bcr} = 1.56$$

$$\theta_{pcr} = \frac{\phi_{cu} - \phi_{bcr}}{m_{cu} - m_{bcr}} = \frac{207.5 - 1.56}{1.86 - 1.56} = 686.5$$

For a simple beam case, the curvature at both ends (Φ_1 and Φ_3) are zero and the curvature at midspan Φ_2 is determined by Eqs. (10)&(16). Since m_s is less than m_{bcr} thus $\phi_2 = m_s$.

$$\Phi_2 = \phi_2\Phi_{cr} = m_s\frac{2\varepsilon_{cr}}{h} = 0.935\frac{2\times 118\times 10^{-6}}{150} =$$

$$= 1.471\times 10^{-6} \text{ mm}^{-1} \ (3.736 \times 10^{-5} \text{ in}^{-1})$$

Finally, the mid span deflection of the beam is calculated by the geometric relationship between curvature and deflection defined in Eq. (29.1)

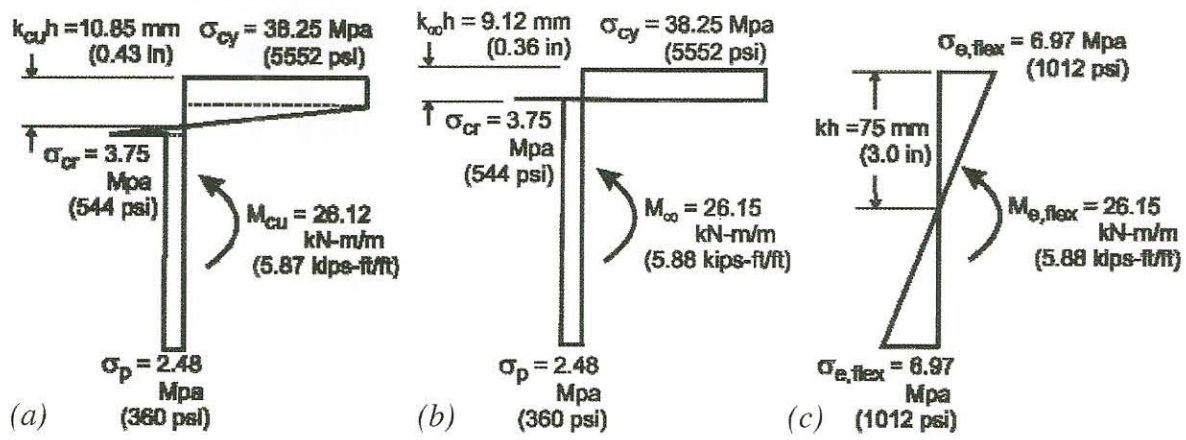

Fig. 9—Stress distribution at ultimate moment: (a) idealized material models at ultimate compressive strain; (b) idealized material models at infinite compressive strain; and (c) elastically equivalent flexural stress.

Short term deflection

$$\delta = \frac{L^2}{96}(\Phi_1 + \Phi_2 + \Phi_3) = \frac{3500^2}{96}\left(1.471\times10^{-6}\right)$$

$$= 0.188 \ mm \ (0.0074 \text{ in})$$

Note that in order to check the deflection limit for each application, long term effects such as creep and shrinkage must be taken into account. This aspect is beyond the scope of this paper.

Stress distributions

In order to demonstrate the differences between the present method and the commonly used elastically equivalent flexural strength $\sigma_{e,flex}$, stress distribution across the beam section at ultimate compressive strain and at infinite strain are compared with the elastic flexural stress. The neutral axis at ultimate compressive strain ε_{cu} of 0.0035, in addition to the ultimate moment are obtained by substituting λ_{cu} = 30 in the expressions for *k* and *m* in range 3 of Table 1.

$$k_{cu} = \frac{2\mu\lambda_{cu}}{-\omega^2 + 2\lambda_{cu}(\omega+\mu) + 2\mu - 1}$$

$$= \frac{2\times0.66\times30}{-10.2^2 + 2\times30(10.2+0.66) + 2\times0.66 - 1} = 0.0723$$

$$k_{cu}h = 0.0723\times150 = 10.85 \ mm$$

$$m_{cu} = \frac{(3\omega\lambda_{cu}^2 - \omega^3 + 3\mu\lambda_{cu}^2 - 3\mu + 2)k_{cu}^2}{\lambda_{cu}^2} - 3\mu(2k_{cu} - 1)$$

$$= \frac{\left(3\times10.2\times30^2 - 10.2^3 + 3\times0.66\times30^2 - 3\times0.66 + 2\right)}{30^2}0.0723^2$$

$$- 3\times0.66(2\times0.0724 - 1)$$

$$= 1.858$$

$$M_{cu} = m_{cu}M_{cr} = 1.858\times14.06 = 26.12 \ kN\text{-}m/m$$

(5.87 KIPS-FT/FT)

The neutral axis parameter and moment at infinite compressive strain are obtained by Eqs. (9), (11)&(12).

$$k_\infty h = \frac{\mu}{\omega+\mu}h = \frac{0.66}{10.2+0.66}\times150 = 9.12 \ mm \ (0.36 \text{ in})$$

$$M_\infty = m_\infty M_{cr} = \frac{3\omega\mu}{\omega+\mu}M_{cr} = \frac{3\times10.2\times0.66}{10.2+0.66}\times14.06$$

$$= 26.15 \ kN\text{-}m/m \ (5.88 \text{ kips-ft/ft})$$

The elastically equivalent flexural strength corresponding to the nominal moment of 26.15 kN-m/m is determined by the flexure formula.

$$\sigma_{e,flex} = \frac{M_u c}{I} = \frac{(26.15\times10^3)\times0.15/2}{1.0\times0.15^3/12}$$

$$= 6.97 \text{ MPa} \qquad (1012 \text{ psi})$$

Stress distributions calculated by the three approaches are compared in Fig. 9. It can be seen that the post crack tensile strength between the idealized material models at ultimate compressive strain (ε_{cu} = 0.0035) and at infinity ($\varepsilon_{cu} = \infty$) are the same at σ_p = 2.48 MPa (360 psi). This level of post crack stress is much smaller than the elastically equivalent flexural strength $\sigma_{e,flex}$ of 6.97 MPa (1012 psi). On the other hand the compressive stress at ultimate strain and at infinity are the same at σ_{cy} = 38.25 MPa (5552 psi) which is much higher than $\sigma_{e,flex}$ of 6.97 MPa (1012 psi). This example points out the inadequacies of several inverse analysis techniques that have been used to obtain residual tensile capacity such as the average residual stress method (ASTM C 1399-04)[35] which report material strengths in terms of equivalent elastic values. Designers should be aware of the shortcomings of these methods and approaches that determine member capacity.

The neutral axis of the idealized model at ultimate compressive strain is slightly higher than the neutral axis at infinity. However, the moment capacities are quite close to one another (26.12 vs. 26.15 kN-m/m). This is due to the elastic stress regions near the neutral axis decreasing while the plastic tensile regions increase.

Acknowledgements

The authors acknowledge the National Science Foundation, programme 0324669-03, Dr P Balaguru, programme manager and Salt River Project for supporting this project.

Conclusions

A design guideline for strain-softening FRC is presented using closed form analytical equations that relate geometrical and material properties to moment and curvature capacity. Conservative reduction factors are introduced for using post crack tensile strength in design and a conversion design chart is proposed for developing FRC systems equivalent to traditional reinforced concretes.

The moment-curvature response for a strain-softening deflection-hardening FRC can be approximated by a bi-linear model while geometric relationship between curvature and deflection can be used for serviceability deflection checks.

REFERENCE

1. ACI (American Concrete Institute), "State-of-the-Art Report on Fibre-Reinforced Concrete," ACI 544.1R-82, 1982. pp. 21

2. Destrée, X., "Concrete Free Suspended Elevated Slabs Reinforced with Only Steel Fibres: Full Scale Testing Results and Conclusions – Design Examples', International Workshop on High Performance Fibre-Reinforced Cementitious Composites in Structural Applications, Honolulu, HI, RILEM Publications SARL, May 2005, pp. 287-294.

3. Soranakom, C.; Mobasher, B.; and Destrée, X., "Numerical Simulation of FRC Round Panel Tests and Full-Scale Elevated Slabs," ACI SP-248-3, Sept. 2007, pp. 31-40.

4. PCI Committee on Glass Fibre-Reinforced Concrete Panels, Recommended Practice for Glass Fibre Reinforced Concrete Panels, third edition, Precast/Prestressed Concrete Institute, 1993, 99 pp.

5. Maalej, M., and Li, V.C., "Flexural/Tensile-Strength Ratio in Engineered Cementitious Composites," Journal of Material in Civil Engineering, V.6, No. 4, Nov. 1994, pp. 513–528.

6. Li, V.C., "On Engineered Cementitious Composites (ECC): A Review of the Material and Its Applications," Journal of Advance Concrete Technology, V. 1, No. 3, Nov. 2003, pp. 215-230.

7. Krstulovic-Opara, N., and Malak, S. "Tensile Behaviour of Slurry Infiltrated Mat Concrete (SIMCON)," ACI Materials Journal, V. 94, No. 1, Jan.-Feb. 1997, pp. 39–46.

8. Bayasi, Z., and Zeng, J., "Flexural Behaviour of Slurry Infiltrated Mat Concrete (SIMCON)," Journal of Materials in Civil Engineering, V. 9, No. 4, Nov. 1997, pp. 194–199.

9. Chanvillard G., and Rigaud, S., "Complete Characterisation of Tensile Properties of Ductal UHPFRC according to the French Recommendations," Proceeding of the 4th International RILEM Workshop, High Performance Fibre-Reinforced Cement Composites (HPFRCC4), Ann Arbor, USA, Jun. 2003, 21-34.

10. Benson, S. D. P., Karihaloo, B. L., "CARDIFRC [registered trademark] -Development and Mechanical Properties. Part I: Development and workability," Magazine of Concrete Research, V. 57, No. 6, Aug. 2005, pp. 347-352.

11. Naaman, A. E., and Reinhardt H. W., "Proposed Classification of HPFRC Composites Based on Their Tensile Response," Materials and Structures, V. 39, No. 289, Jun. 2006, pp. 547–555.

12. Vandewalle, L. et al. "Test and Design Methods for Steel Fibre-Reinforced Concrete. Recommendations for Bending Test," Materials and Structures, V. 33, No. 225, Jan. 2000a, pp. 3-5.

13. Vandewalle, L. et al., "Test and Design Methods for Steel Fibre-Reinforced Concrete: Recommendations for σ-ε Design Method," Materials and Structures, V. 33, No. 226, Mar. 2000b, pp. 75-81.

14.Vandewalle, L. et al., "Design of Steel Fibre-Reinforced Concrete Using the s-w Method: Principle and Applications," Materials and Structures, V. 35, No. 249, Jun. 2002a, pp. 262-278.

15. Vandewalle, L. et al., "Test and Design Methods for Steel Fibre Reinforced Concrete - Final Recommendation," Materials and Structures, V. 35, No. 253, Nov. 2002b, pp. 579-582.

16. Vandewalle, L. et al. "Test and Design Methods for Steel Fibre Reinforced Concrete-s-e Design Method - Final Recommendation," Materials and Structures, V. 36, No. 262, Oct. 2003, pp. 560-567.

17.Teutsch, M., "German Guidelines on Steel Fibre Concrete," Proceeding of the North American/European Workshop on Advances in Fibre Reinforced Concrete, BEFIB 2004, Bergamo, Italy, Sept. 2004, pp. 23-28.

18. Barr B., and Lee, M.K., "FRC Guidelines in the UK, with Emphasis on SFRC in Floor Slabs," Proceeding of the North American/European Workshop on Advances in Fibre Reinforced Concrete, BEFIB 2004, Bergamo, Italy, Sept. 2004, pp. 29-38.

19. Japan Society of Civil Engineers JSCE-SF4., "Methods of Tests for Flexural Strength and Flexural Toughness of Steel Fibre Reinforced Concrete," Concrete Library International, Part III-2, 3, 1984, pp. 58-61.

20. di Prisco, M.; Toniolo, G.; Plizzari, G. A.; Cangiano, S.; and Failla, C., "Italian Guidelines on SFRC," Proceeding of the North American/European Workshop on Advances in Fiber Reinforced Concrete, BEFIB 2004, Bergamo, Italy, Sept. 2004, pp. 39–72.

21. Swamy, R.N.; Mangat, P.S.; and Rao, C.V.S.K., "The Mechanics of Fibre Reinforced Cement Matrices," Fiber Reinforced Concrete ACI SP-44, 1975, pp. 1-28.

22. Fischer, G. "Current U.S. Guidelines on Fibre Reinforced Concrete and Implementation in Structural Design," Proceeding of the North American/European Workshop on Advances in Fibre Reinforced Concrete, BEFIB 2004, Bergamo, Italy, Sept. 2004, pp. 13-22.

23. Henager, C.H., and Doherty, T.J., "Analysis of Reinforced Fibrous Concrete Beams," Proceedings, ASCE. V.12 ST-1, pp. 177-188.

24. ACI Committee 318, Building Code Requirements for Structural Concrete, ACI Manual of Concrete Practice, American Concrete Institute, Detroit, 2005.

25. Soranakom, C., and Mobasher, B., "Closed-Form Solutions for Flexural Response of Fibre-Reinforced Concrete Beams," Journal of Engineering Mechanics, V. 133, No. 8, Aug. 2007, pp. 933-941.

26. Soranakom, C., and Mobasher, B., "Development of Design Guidelines for Strain Softening Fibre Reinforced Concrete," 7th RILEM International Symposium on Fibre Reinforced Concrete, BEFIB 2008, Chennai (Madras), India, Sept. 2008, pp. 513-523.

27. Swamy R.N., Al-Ta'an S.A. "Deformation and Ultimate Strength in Flexural of Reinforced Concrete Beams Made with Steel Fibre Concrete," ACI Structural Journal, Vol. 78, No. 5, Sept. - Oct. 1981, pp. 395-405.

28. Hassoun M.N., Sahebjam K. "Plastic Hinge in Two-Span Reinforced Concrete Beams Containing Steel Fibres," Prc., Can. Soc. For Civ. Engrg. 1985, pp. 119-139.

29. Soranakom C., "Multi-Scale Modeling of Fibre and Fabric Reinforced Cement Based," Ph.D. Dissertation, Arizona State University, Tempe, USA, 2008.

30. Soranakom, C., and Mobasher, B., "Closed Form Solutions for Flexural Response of Hybrid Reinforced Concrete Beams: Part II - Experimental Verifications," ASCE Journal of Structural Engineering (Manuscript in review)

31. Kwak Y.-K., Eberhard, M.O., Kim, W.-S., and Kim, J., "Shear Strength of Steel Fibre-Reinforced Concrete Beams without Stirrups," ACI Structural Journal, V.99, No.4, July-August, 2002, pp. 530-538.

32 Parra-Montesinos, G., "Shear Strength of Beams with Deformed Steel Fibres-Evaluating an Alternative to Minimum Transverse Reinforcement," Concrete International, November, 2006, pp. 57-66.

33. Ghali, A., "Deflection of Reinforced Concrete Members: A Critical Review," ACI Structural Journal, V. 90, No. 4, July-August, 1993, pp. 364-373.

34. Ghali, A., and Favre, R., Concrete Structures: Stresses and Deformations, Chapman and Hall, London, 1986, 352 pp.

35. Dupont D., "Modelling and Experimental Validation of the Constitutive Law (s-e) and Cracking Behaviour of Steel Fibre Reinforced Concrete" Ph.D. Dissertation, Catholic, University of Leuven, Belgium, 2003.

36. ASTM C 1399-04, "Standard Tests Method for Obtaining Average Residual-Strength of Fibre-Reinforced Concrete," ASTM International, PA, 2004, 6 pp.